PERGAMON

International Journal of Heat and Mass Transfer 45 (2002) 1905–1914

International Journal of HEAT and MASS TRANSFER

www.elsevier.com/locate/ijhmt

Analytical solutions of the 1-D heat conduction problem for a single fin with temperature dependent heat transfer coefficient – II. Recurrent direct solution

I.N. Dul'kin *, G.I. Garas'ko

All-Russian Electrical Engineering Institute, 12 Krasnokazarmennaya Street, 111250 Moscow, Russia

Received 11 January 2001; received in revised form 22 June 2001

Abstract

The recurrent direct solution of the 1-D heat conduction problem for a single straight fin and spine with power-law-type temperature dependent heat transfer coefficient has been derived using inversion of the closed-form solution obtained in the first part of the study. The expression with improving convergence to calculate accurately the dimensionless temperature excess T_e at the fin tip for a given values of the fin parameter N and exponent n in heat transfer equation has been obtained by a linearization method. Equation for the temperature excess distribution throughout the fin has also been derived. The obtained formula for T_e allows to calculate the fin base thermal conductance and augmentation factor. Obtained expressions are seen to be simple and convenient for the engineering design of the fins and finned surfaces.

1. Introduction

Closed-form solution of 1-D heat conduction problem for a single straight fin and spine of constant cross-section has been obtained in the first part of the study [1]. This solution is expressed in the ordinary but not special or hypergeometric functions. However, it has an "inverse" form (i.e., dependence of the fin convective–conductive parameter N on the dimensionless fin tip temperature excess T_e and exponent n in the heat transfer equation).

The objective of the present second part of the study is to determine the direct dependence T_e on N for given n. A simple recurrent formula is derived by inversion of the obtained closed-form expression. Its linearization results in increase of the convergence rate. A generalized expression for definite integral with respect to T depending on bottom limit of integration only (for given n) is found. The closed-form and recurrent expressions to determine the temperature distribution along a fin are derived on the basis of this generalized expression. The range of applicability of the obtained solution and its relative deviation from the data of the numerical integration are considered. In addition, special cases with negative exponent n are investigated more thoroughly taking into account the existence of the instability and non-single valued solutions.

Equations intended for the evaluation of the fin base thermal conductance and augmentation factor (effectiveness) are obtained using the derived formula for T_e. Therefore, the results of this investigation make possible fast and simple heat transfer evaluation of the fins and finned surfaces. The examples of this type evaluation are presented and their results are compared with the theoretical and experimental data in the related literature.

2. Theoretical analysis

Closed-form inverse Eq. (18) from the first part of the study [1] for given values of n and T_e can be expressed as follows:

$$N = T_e^{-0.4n}\operatorname{arcosh}(1/T_e), \tag{1}$$

* Corresponding author.

0017-9310/02/$ - see front matter
PII: S0017-9310(01)00285-X

Nomenclature

A	cross-section area of the fin (m^2)
A_z	dimensionless function defined in Eq. (6)
a	given constant in Eq. (26) ($W\ m^{-2}\ K^{-(n+1)}$)
E_f	fin augmentation factor (effectiveness)
E_t	finned tube augmentation factor
G_b	dimensionless thermal conductance for the fin base at given n
g_b	thermal conductance for the fin base at given n ($W\ K^{-1}$)
G_b^*	dimensionless thermal conductance for the fin base at given n corresponding to N^* and T_e^*
$G_{b,0}$	dimensionless thermal conductance for the fin base at $n = 0$
G_d	relative thermal conductance for the fin base at given n
$G_{d,\infty}$	relative thermal conductance for the "asymptotical" fin base
h	heat transfer coefficient ($W\ m^{-2}\ K^{-1}$)
h_b	heat transfer coefficient for the fin base ($W\ m^{-2}\ K^{-1}$)
j	iteration number in the solution of the recurrent Eq. (4)
k	thermal conductivity of the fin material ($W\ m^{-1}\ K^{-1}$)
l	fin height (m)
n	given exponent in Eq. (26)
N	dimensionless fin parameter defined under Eq. (1)
N^+	fin parameter corresponding to $T_e = 0$ for $-1 \leqslant n < 0$
N^*	fin parameter corresponding to maximum of the N vs T_e curve at $n < -1$
P	circumference of the fin cross-section area (m)
t	temperature of the fin (°C)
t_a	temperature of the ambient fluid surrounding the fin (°C)
T	dimensionless temperature excess of the fin
T_e	dimensionless temperature difference between the fin tip and ambient fluid
T_e^*	dimensionless temperature difference between the fin tip and ambient fluid corresponding to N^* for $n < -1$
x	space coordinate (m)
X	dimensionless space coordinate
Z	dimensionless function defined in Eq. (5)

Greek symbols

Δ	increment of T_e in Eqs. (A.1) and (A.2)
δ	thickness of the fin (m)
ϑ	temperature difference between a fin and ambient fluid (°C)
φ	relative deviation (%)

Subscripts and superscripts

a	refers to the ambient fluid
b	refers to the fin base ($X = 1$)
e	refers to the fin tip ($X = 0$)
∞	refers to the fin with infinite height $l = \infty$

where $N = l\sqrt{a\vartheta_b^n P/(kA)}$ is the convective–conductive parameter of a fin, $T_e = \vartheta_e/\vartheta_b$ is the dimensionless temperature excess at the fin tip. However, the value of T_e is usually unknown. The fin convective–conductive parameter N and exponent n in the heat transfer equation are prescribed according to the statement of the problem. Therefore, the task is to find an expression intended for determination of T_e at given values of N and n. Such expression can be easily derived from Eq. (1) directly in the following recurrent form:

$$T_e = \frac{1}{\cosh(NT_e^{0.4n})}. \tag{2}$$

For $n = 0$ this equation transforms into the well-known formula

$$T_e = \frac{1}{\cosh N}. \tag{3}$$

Unfortunately, Eq. (2) has a poor convergence. Therefore, using the linearization method it has been transformed into the following recurrent formula which allows to get accurate solution after a small number of iterations:

$$T_e = \frac{1 + A_z}{\cosh Z + (A_z/T_e)}, \tag{4}$$

where

$$Z = NT_e^{0.4n}, \tag{5}$$

and

$$A_z = 0.4nZ \tanh Z. \tag{6}$$

Derivation of this formula is given in Appendix A. An arbitrary value of T_e in the range $0 < T_e \leqslant 1$, for instance $T_e = 0.8$ can be taken as a zeroth approximation in the RHS of Eq. (4). 2–3 iterations are enough to obtain a convergence between two successive iterations of Eq. (4) with the accuracy better than 0.1%.

Plots of T_e vs N for different n calculated by the numerical integration of Eqs. (12) and (13) in the first part [1] (solid lines) and by recurrent Eq. (4)

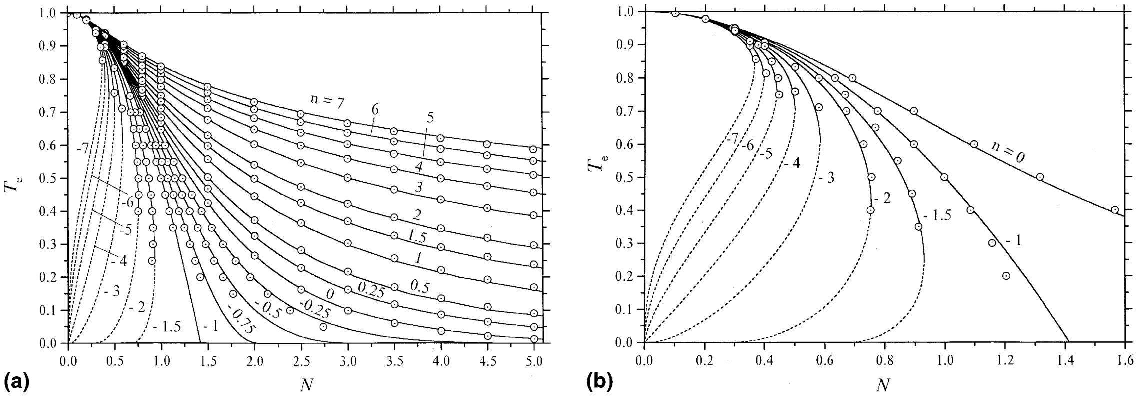

Fig. 1. The set of curves T_e vs N obtained by the numerical integration for positive and negative values of n (a) and in increased scale for negative n (b). Solid lines correspond to stable or physically realizable states. Dashed lines relate to unstable states with negative values of n. Dot-centered open circles represent data obtained with the help of formulae (4)–(6).

(dot-centered open circles) are presented in Figs. 1(a) and (b). It is seen that results calculated by simple formulae (4)–(6) coincide closely with the numerical ones (accuracy of the calculations using Eqs. (4)–(6) is discussed in Section 2.1). As can be seen from Fig. 1(b) the results of the calculation using the recurrent formula (4) for negative $-1 \leqslant n < 0$ are close to the numerical ones for $T_e \geqslant 0.1$–0.2 that corresponds to $N < N^+$. For negative $-7 \leqslant n < -1$ a good agreement can be seen between results of the approximate and numerical calculations on the physically stable branches of the curves T_e vs N. Physically unstable branches of these curves can be calculated only for given n and T_e numerically and by the inverse formula (1). Numerical results are plotted in Figs. 1(a) and (b) by short dashed lines.

2.1. The relative accuracy of the recurrent formula compared to results of the numerical integration

Relative deviation φ of the T_e vs N curves calculated by recurrent Eqs. (4)–(6) and by numerical integration of Eqs. (12) and (13) in [1] for given negative (dotted lines) and positive values of n is presented in Fig. 2. Dashed lines are used for $0 \leqslant n \leqslant 0.6$ and solid lines for $1 \leqslant n \leqslant 7$ accordingly. From this plot it can be seen that the condition $\varphi < \pm 1\%$ holds in a wide range of T_e both for negative and positive n. Fig. 3 presents the level lines of the relative deviation for $\varphi = 0.5\%$, 1%, 2% and 4%. These lines are plotted according to data presented in Fig. 2 for practically most important range of positive $0 < n \leqslant 4$ and $N < 6$.

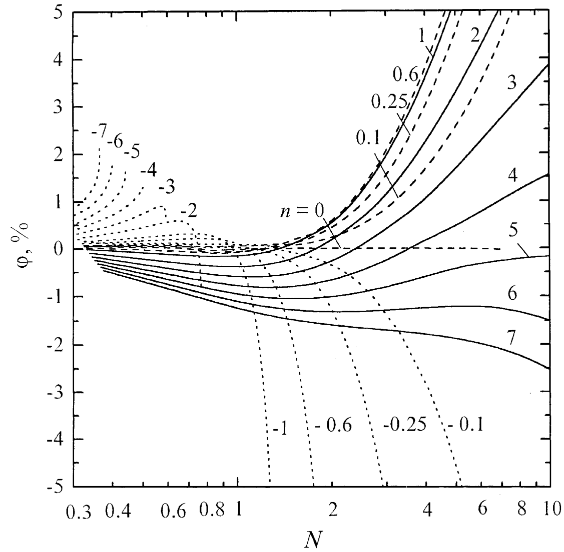

Fig. 2. Relative deviation φ of the T_e vs N curves calculated with formulae (4)–(6) and by numerical integration for negative (dotted lines) and positive values of n. Dashed lines are used for $0 \leqslant n \leqslant 0.6$ and solid lines for $1 \leqslant n \leqslant 7$.

2.2. The temperature distribution along a fin

According to the preceding results, the integral in Eqs. (12) and (13) in the first part of the study [1] can be expressed in a closed-form with respect to T_e and n in ordinary but not hypergeometric or other special function form in a wide range of T_e for $-7 \leqslant n \leqslant +7$ (see Eq. (1)). To determine the temperature distribution along a fin for the given values of T_e and n, Eq. (8) [1] can be used. This equation includes the same integral as Eq. (12) [1] but in other limits of integration (from T_e to T instead of from T_e to 1). The first goal of this paragraph is to obtain a general expression for evaluation of the considered definite integral with an arbitrary upper limit. To do this, it is suitable to introduce another variable of integration. Denote $\xi = T_e/T$. Using the

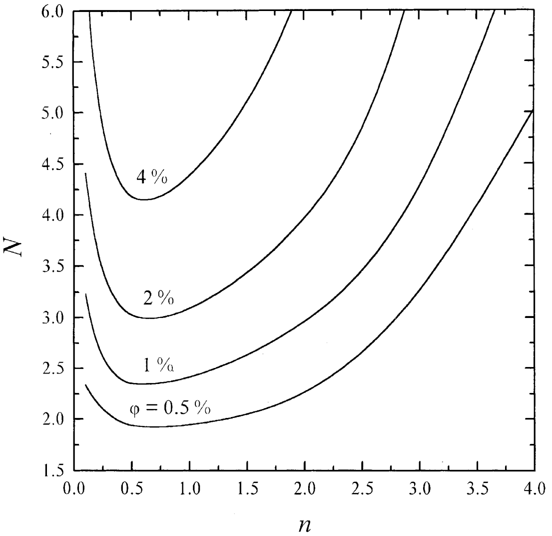

Fig. 3. Dependent of the fin parameter N on exponent n for given relative deviation φ of the function T_e vs N calculated using formulae (4)–(6) and by numerical integration for positive $0 < n \leqslant 4$.

simple transformations of the integral in Eq. (12) [1], we obtain the following expression:

$$N = \int_{T_e}^{1} \frac{\sqrt{(n+2)/2}\,\mathrm{d}T}{\sqrt{T^{n+2} - T_e^{n+2}}} = -\int_{1}^{T_e} \frac{\sqrt{(n+2)/2}\,\mathrm{d}\xi}{\xi\sqrt{(T_e/\xi)^n(1-\xi^{n+2})}} = \sqrt{\frac{n+2}{2T_e^n}} \int_{T_e}^{1} \frac{\mathrm{d}\xi}{\sqrt{\xi^{2-n} - \xi^4}}, \quad n \neq -2. \tag{7}$$

According to Eq. (1) the above expression is equal to $\mathrm{arcosh}(1/T_e)/T_e^{0.4n}$. By equating these expressions we obtain:

$$I(T_e; n) = \int_{T_e}^{1} \frac{\mathrm{d}\xi}{\sqrt{\xi^{2-n} - \xi^4}} = T_e^{n/2}\sqrt{\frac{2}{n+2}} \frac{\mathrm{arcosh}(1/T_e)}{T_e^{0.4n}}. \tag{8}$$

An integral in LHS of Eq. (8) for given parameter n depends on the bottom limit of integration T_e only. Therefore in general case denoting in the integral of Eq. (8) the bottom limit of integration by τ we get the following generalized expression:

$$I(\tau; n) \equiv \int_{\tau}^{1} \frac{\mathrm{d}\xi}{\sqrt{\xi^{2-n} - \xi^4}} = \tau^{n/2}\sqrt{\frac{2}{n+2}} \frac{\mathrm{arcosh}(1/\tau)}{\tau^{0.4n}}. \tag{9}$$

So, the integral in Eq. (8) [1] can be expressed in a form:

$$X \cdot N = \int_{T_e}^{T} \frac{\sqrt{(n+2)/2}\,\mathrm{d}T}{\sqrt{T^{n+2} - T_e^{n+2}}} = \sqrt{\frac{n+2}{2T_e^n}} \int_{T_e/T}^{1} \frac{\mathrm{d}\xi}{\sqrt{\xi^{2-n} - \xi^4}} = \sqrt{\frac{n+2}{2T_e^n}} I(T_e/T; n), \tag{10}$$

where $X = x/l$, x is a space coordinate. After T_e is determined using formulae (4)–(6) the temperature distribution along a fin can be obtained by Eq. (10) in an inverse form. An integral in RHS of Eq. (10) according to Eq. (9), where $\tau = T_e/T$ can be expressed as:

$$I(T_e/T; n) = \int_{T_e/T}^{1} \frac{\mathrm{d}\xi}{\sqrt{\xi^{2-n} - \xi^4}} = \sqrt{\frac{2}{n+2}} \left(\frac{T_e}{T}\right)^{n/2} \frac{\mathrm{arcosh}[(1/(T_e/T)]}{(T_e/T)^{0.4n}}. \tag{11}$$

Substituting this equation in Eq. (10) we get a simple expression for the temperature distribution along a fin in an inverse form

$$X = \mathrm{arcosh}[1/(T_e/T)]/[NT^{n/2}(T_e/T)^{0.4n}]. \tag{12}$$

Eq. (12) can be easy transformed into the recurrent expression to determine T for given n and N with T_e obtained using Eqs. (4)–(6). As a result we get

$$T = T_e \cosh(NXT_e^{0.4n} T^{0.1n}). \tag{13}$$

This equation has a sufficiently high rate of convergence (it is enough 1–3 iterations for $X \leqslant 0.4$ and 4–8 iterations for $0.4 < X \leqslant 0.9$ and arbitrary values of n and N).

The temperature profiles throughout the fin with insulated tip according to our evaluations using Eq. (12) and Eqs. (4)–(6) to calculate T_e are displayed in Fig. 4. Comparison of the profiles evaluated in [5] using exact hypergeometric formula for $N = 1$ and $n = -0.25$, 0.25, 2, 3 (dot-centered open circles) with our profiles (solid lines) for corresponding values of n shows that they practically coincide. Comparison between the results of our temperature profile evaluation using Eq. (13) in combination with Eqs. (4)–(6) to calculate T_e and experimental data is presented in Fig. 5. The experiments have been performed for cylindrical copper rods in nucleate pool boiling with R113 [4] and in film pool boiling with water [5]. The fin dimensions and values of n and N parameters corresponding to these boiling modes and dimensions are given in the caption of Fig. 5. The details of experiments are available in [4,5]. It can be seen that our analytical temperature profile evaluation agrees well with the experimental data [4,5], in the latter case for two values of the fin base temperature excess.

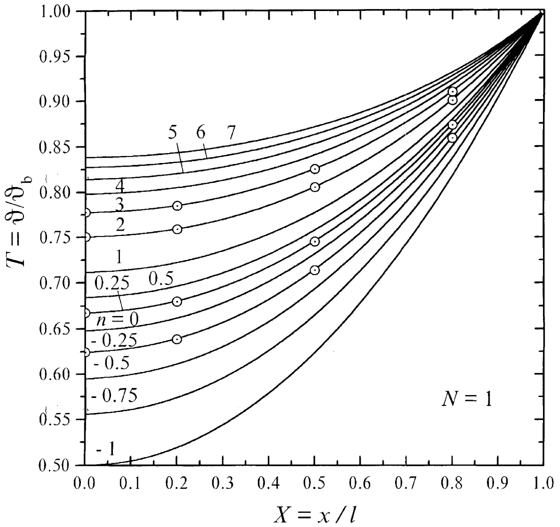

Fig. 4. Dimensionless temperature excess profiles for the fins with insulated tip predicted using Eqs. (12) and (4)–(6) (solid lines) or the exact hypergeometric formula in [5] (dot-centered open circles). All profiles evaluated for the fin parameter $N = 1$ and different values of exponent n.

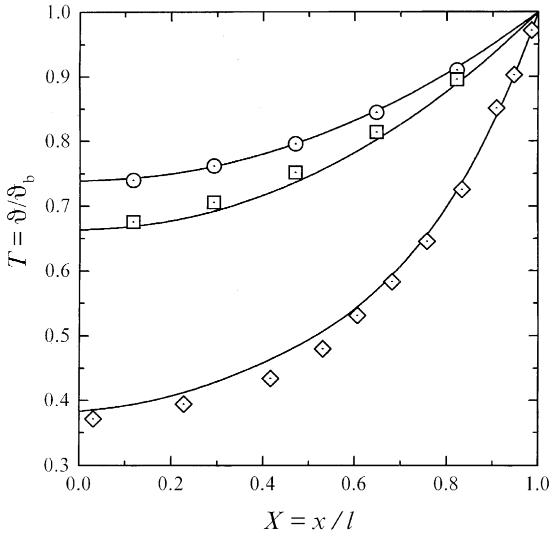

Fig. 5. Comparison of the dimensionless temperature excess profiles for the cylindrical copper rods with insulated tip predicted by formulae (13) and (4)–(6) (solid lines) with measured ones. The dot-centered open diamonds present the experimental data from [4] in nucleate pool boiling with R113 ($n = 2$) on the rod of $d = 14$ mm and $l = 66$ mm, at $\vartheta_b = 17.5$ °C ($N = 3.47$). The dot-centered open circles and squares relate to the experimental data from [5] in film boiling with water ($n = -0.5$) on the rod of $d = 25$ mm and $l = 85$ mm for $\vartheta_b = 140$ °C ($N = 0.7$) and $\vartheta_b = 254$ °C ($N = 0.9$), respectively.

3. Thermal conductance at the base of a fin

The dimensionless thermal conductance at the base of a fin (the input thermal admittance according to parametrization proposed by Kraus et al. [6]) G_b can be determined by means of Eq. (10) ($n \neq -2$) or Eq. (11) ($n = -2$) in [1]. The fin tip temperature excess T_e is calculated using the recurrent formula (4) in combination with Eqs. (5) and (6). The results of such calculation are shown in Fig. 6 by dot-centered open circles, whereas the results of analogous calculation using the values of T_e determined by numerical integration are presented in the same figure by solid lines (at stable states for all n) or by dashed lines (for unstable states, at $n < -1$). The G_b calculation based on the values of T_e determined by Eqs. (4)–(6) or by the numerical integration agree well with each other. The analytical solution for T_e at $n = 0$ is expressed by Eq. (3). Substituting this solution into Eq. (10) [1] we get the expression for the fin base thermal conductance for uniform surface heat transfer coefficient

$$G_{b,0} = N\sqrt{1 - (1/\cosh N)^2} = N \tanh N. \tag{14}$$

Getting the quotient of the input fin thermal conductance (at base) for an arbitrary value of the exponent n to that for $n = 0$, the following expression for the relative fin base thermal conductance can be obtained:

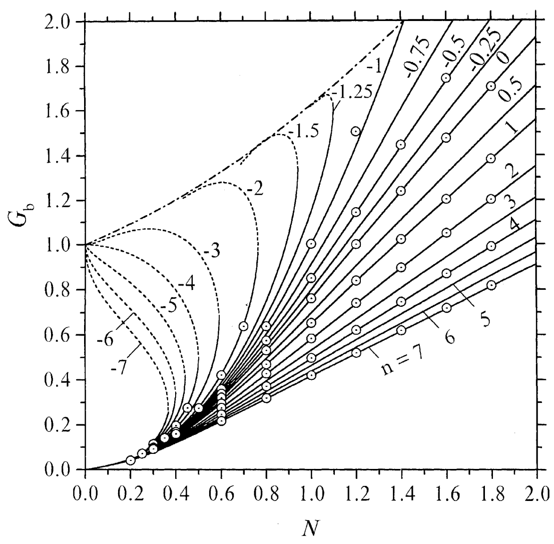

Fig. 6. The fin base thermal conductance G_b vs the fin parameter N for different values of the exponent n. Solid lines correspond to the stable states and short dashed lines to the physically not realizable states for $n < -1$. The top envelope of the latter is shown by dot-dashed line. Dot-centered open circles relate to analytical predictions obtained using Eqs. (10) and (11) [1] for $n \neq -2$ and for $n = -2$, respectively, in combination with Eqs. (4)–(6) to calculate T_e.

$$G_d = \frac{G_b}{G_{b,0}} = \frac{\sqrt{[2/(n+2)](1-T_e^{n+2})}}{\tanh N}, \quad n \neq -2, \tag{15}$$

$$G_d = \frac{\sqrt{2\ln(1/T_e)}}{\tanh N}, \quad n = -2. \tag{16}$$

For so called asymptotical fins, i.e., fins with an infinite height $N \to \infty$, the value of $\tanh N = 1$, $T_e = 0$ and the relative thermal conductance can be written as follows:

$$G_{d,\infty} = \sqrt{\frac{2}{n+2}}. \tag{17}$$

The dependence of G_d on the fin parameter N varying in the range 0–2 for given negative and positive values of the exponent n is shown in Figs. 7(a) and (b), respectively. The results of numerical integration are displayed by solid lines and analytical results obtained using formulae (4)–(6) and (15), (16) by dot-centered open circles. Close agreement is clearly seen for analytical and numerical results in the whole range of N and n. Only physically stable (realizable) branches of the curve are shown in Fig. 7(a) for $n < -1$. The boundary of these states is shown in Fig. 7(a) by a short dashed line. For $-1 \leqslant n < 0$ this boundary corresponds to $T_e = 0$. All curves G_d vs N in Fig. 7(b) tend to the asymptotical values of $G_d = G_{d,\infty}$ defined by Eq. (17) for $n > 0$.

3.1. Distinctive features of the solution for $n < 0$

We have pointed out in [1] some features of the curves N vs T_e for $n < 0$ in the ranges $-7 \leqslant n \leqslant -1$ and $-1 < n < 0$. Consider now Fig. 1(b), where the dependence T_e vs N is displayed in a large scale for $n \leqslant 0$. Here, as well as in Fig. 1(a), results obtained by numerical integration of Eqs. (12) and (13) in [1] for physically stable regions are shown by solid lines and the data calculated using formulae (4)–(6) by dot-centered open circles. The physically unstable branches of these curves are plotted by short dashed lines. The unstable portions appear for $n < -1$. A value $T_e^* = 0$ corresponds to $N^* = \sqrt{2}$ for $n = -1$. In the region $n < -1$ the "critical" value of N^* reduces and corresponding value of T_e^* increases with decreasing n. Plots of these critical values and corresponding value of the fin base conductance G_b^* against exponent n obtained using numerical integration are shown in Fig. 8 by dot-centered open circles. To simplify calculations, these relationships have been approximated by the following analytical formulae:

$$T_e^* = 2^{m_1}, \tag{18}$$

$$N^* = 2^{m_2}, \tag{19}$$

$$G_b^* = 2^{m_3}, \tag{20}$$

where

$$m_1 = 1/(0.4 + 0.6n), \tag{21}$$

$$m_2 = 0.5 - 4\varsigma + 3.71\varsigma^2 - 2\varsigma^3, \tag{22}$$

$$m_3 = 1 - 3.349\varsigma + 0.154\varsigma^2 - 0.18\varsigma^3, \tag{23}$$

$$\varsigma = \log(-n). \tag{24}$$

The approximation curves displayed in Fig. 8 by the solid lines lie very close to the results of the numerical integration.

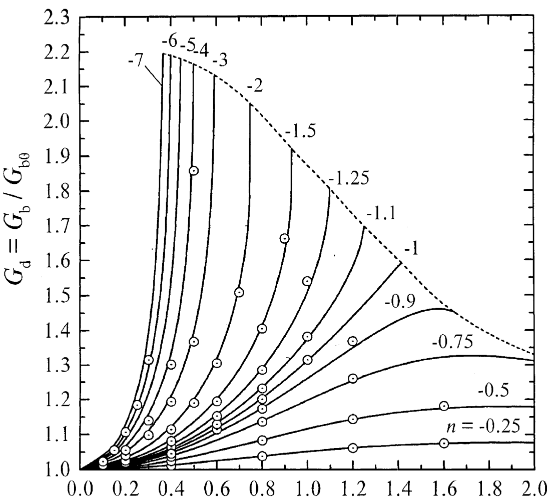

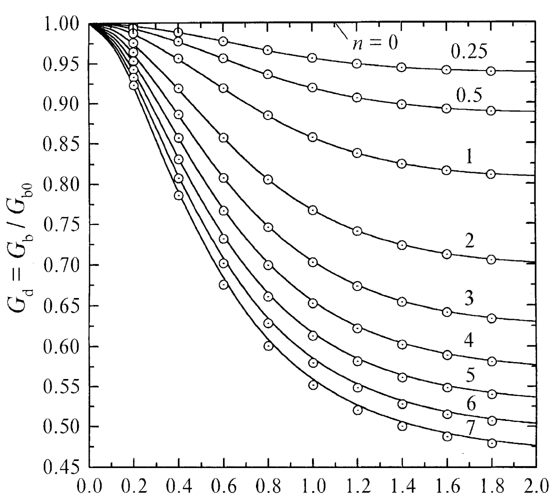

Fig. 7. The relative dimensionless fin base conductance G_d vs the fin parameter N for negative (a) and positive (b) values of the exponent n calculated numerically (solid lines) and obtained by Eqs. (15) and (16) in accordance with Eqs. (4)–(6) (dot-centered open circles). Short dashed curve corresponds to the limiting values of N and G_d for negative n.

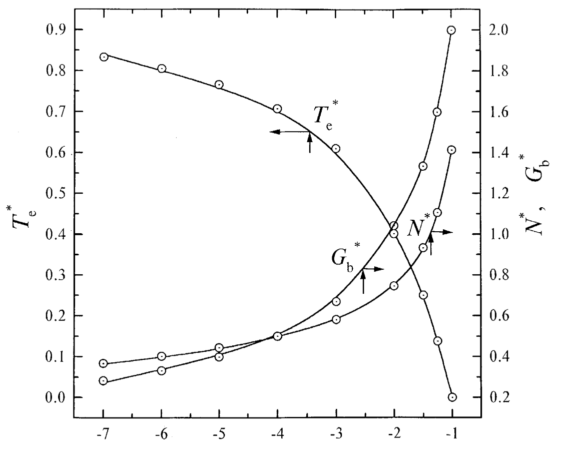

Fig. 8. The limiting values of N^*, T_e^* and G_d^* for different $-7 \leqslant n \leqslant -1$ corresponding to the maximum value of N in Fig. 1 for given n.

Consider now the analytical expressions for the "limiting" values of the fin parameter N^+ at the intersection of the curve T_e vs N for given $-1 \leqslant n < 0$ with the abscissa axis ($T_e = 0$). Substituting zero value of T_e in the integrand and bottom limit of integration in Eq. (12) [1], we get

$$N^+ = \frac{\sqrt{2(n+2)}}{|n|}. \tag{25}$$

The plot of this function is shown on the right ordinate axis in Fig. 9. Corresponding values of the relative fin base conductance G_d^+ obtained with formulae (10) [1]

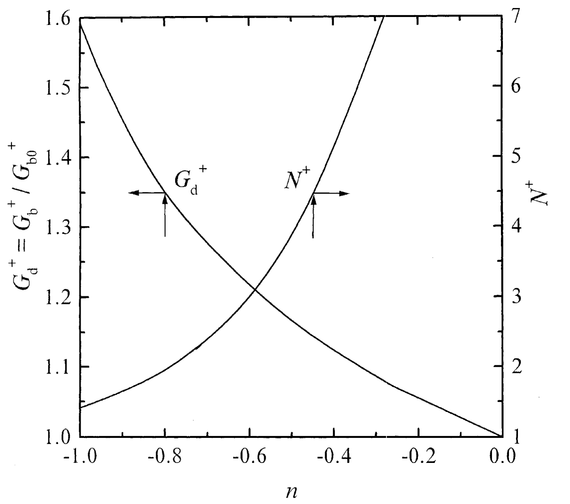

Fig. 9. The limiting values of N^+ and G_d^+ for different $-1 \leqslant n \leqslant 0$. The value of $T_e = 0$ corresponds to these values of N^+ and G_d^+.

and (15) are shown on the left ordinate axis of the same figure.

4. A numerical example

Let us consider a copper finned tube with longitudinal straight fins of rectangular profile from the numerical example of Ünal's paper [7] (thermal conductivity of the copper $k = 380$ W m^{-1} K^{-1}) with a single mode of heat transfer from the outer surface of the tube and fins. A nucleate pool boiling heat transfer to saturated R113 at atmospheric pressure is analyzed ($n = 2$). Similarly to [7], we assume that heat transfer equation has the form

$$h = 12.1\vartheta^2 \tag{26}$$

with the following assumptions:

- The wall superheat on the outer surface of the tube is equal to that of the fin bases $\vartheta_b = 13K$ and is uniform over the tube circumference.
- The tube curvature under the fins is neglected and the system is considered to be a plane wall with longitudinal fins.
- The Biot number for any fin on the tube is much smaller than 0.1, which justifies utilization of the 1-D heat conduction model.

The geometrical dimensions of the analyzed finned tube and fins are given in Table 1. The procedure of solution will be considered in detail for the following input data:

- Fin thickness $\delta = 0.2$ mm.
- Fin height $l = 2.5$ mm.
- Distance between two successive fins on the outer surface of a tube $s = 1$ mm.

4.1. Solution procedure

(1) The heat transfer coefficient at the fin base can be defined by above Eq. (26) for nucleate pool boiling of R113 and given $\vartheta = 13$ K

$$h = 12.1\vartheta^2 = 12.1 \times 13^2 = 2044.9 \text{ W m}^{-2} \text{ K}^{-1}.$$

(2) The quotient P/A for the longitudinal straight fin of rectangular profile (constant thickness) is equal to $2/\delta$. Therefore, according to Eq. (3) [1], the convective–conductive fin parameter is determined as follows:

$$N = l\sqrt{h_b P/(kA)} = l\sqrt{2h_b/(k\delta)}$$
$$= 2.5 \times 10^{-3}\sqrt{2 \times 2044.9/(380 \times 0.2 \times 10^{-3})} = 0.58.$$

(3) A dimensionless fin tip temperature difference T_e is recurrently determined for given $n = 2$ and fin parameter $N = 0.58$ obtained above through the use of Eqs. (4)–(6). As zeroth approximation T_e is assumed to be 0.8. Then using Eqs. (5) and (6), we get

$$Z = NT_e^{0.4n} = 0.58 \times 0.8^{0.4\times2} = 0.58 \times 0.8^{0.8} = 0.4852,$$

Table 1
Finned tube augmentation factor E_t for given values δ, l and s

δ (mm)	l (mm)	N	T_e	G_b	E_f	Factor E_t for s (mm)		
						1	2	3
0.2	2.5	0.58	0.8775	0.2616	19.445	4.074	2.677	2.153
	5.0	1.16	0.7087	0.7092	26.358	5.226	3.305	2.585
	7.5	1.74	0.5830	1.1570	28.667	5.611	3.515	2.729
0.4	2.5	0.41	0.9300	0.1455	10.815	3.804	2.636	2.155
	5.0	0.82	0.8025	0.4436	16.486	5.425	3.581	2.822
	7.5	1.23	0.6900	0.7648	18.950	6.129	3.992	3.112
0.6	2.5	0.33	0.9500	0.1020	7.583	3.469	2.519	2.097
	5.0	0.67	0.8490	0.3284	12.205	5.202	3.586	2.867
	7.5	1.01	0.7500	0.5875	14.558	6.084	4.129	3.260

$$A_z = 0.4nZ\tanh Z = 0.4\times 2\times 0.4852\tanh 0.4852 = 0.1748$$

and using Eq. (4) we get the first approximation for T_e

$$T_e^{(1)} = (1+A_z)/[\cosh Z + (A_z/T_e^{(0)})] = (1+0.1748)/[\cosh 0.4852 + (0.1748/0.8)] = 0.8777.$$

Repeating the above procedure with a new value of $T_e = T_e^{(1)} = 0.8777$ in RHS of Eq. (4) we have

$$Z = 0.58\times 0.8777^{0.8} = 0.5225,$$

$$A_z = 0.8\times 0.5225\times\tanh 0.5225 = 0.2005$$

and

$$T_e^{(2)} = (1+0.2005)/[\cosh 0.5225 + (0.2005/0.8777)] = 0.8775.$$

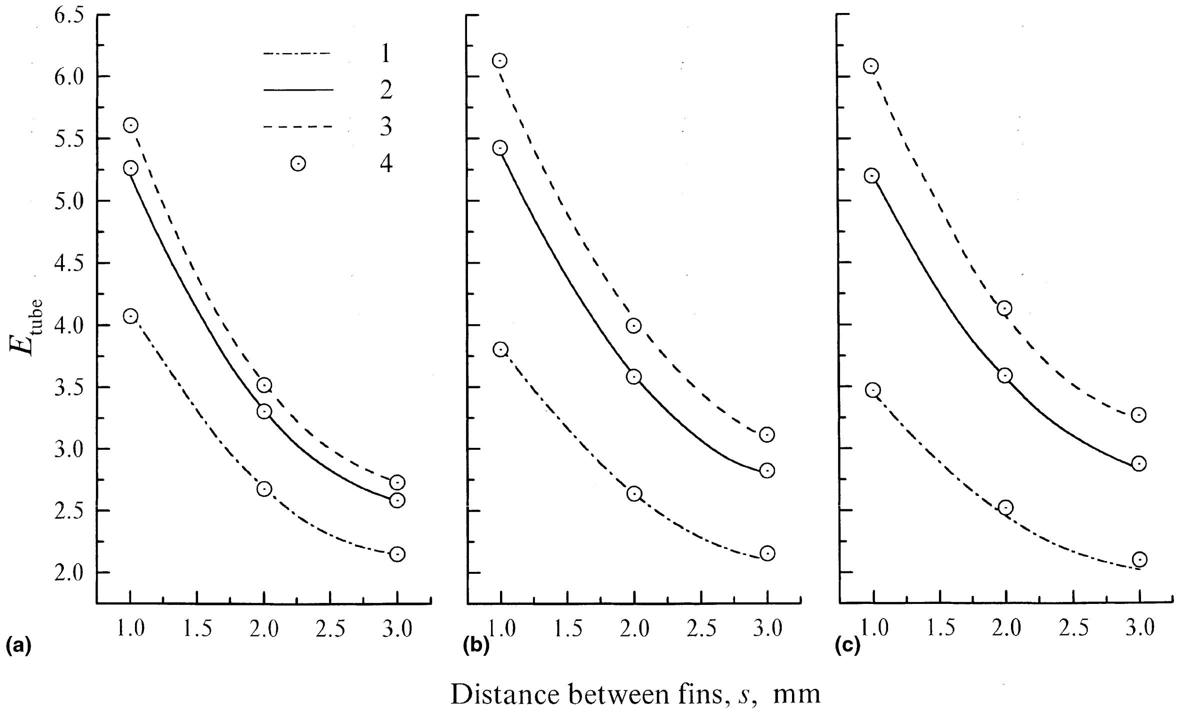

Fig. 10. Dependence of the finned tube augmentation factor E_t on the distance between successive fins s for the fin thickness values $\delta = 0.2$ mm (a), 0.4 mm (b) and 0.6 mm (c) and fin height $l = 2.5$ mm (1), 5 mm (2) and 7.5 mm (3) according to Ünal's results and our estimation for the same parameter values (4).

The third approximation gives $T_e^{(3)} = T_e^{(2)} = 0.8775$. This value is assumed to be the final value of T_e.

(4) A dimensionless thermal conductance of the fin base can be found using Eq. (10) [1] and the obtained value of T_e

$$G_b = N\sqrt{[2/(n+2)](1 - T_e^{n+2})} = 0.58\sqrt{[2/(2+2)](1 - 0.8775^4)} = 0.2616.$$

(5) A fin augmentation factor (fin effectiveness according to Gardner's definition [2] and [3]) we can estimate using following equation:

$$E_f = g_b/(h_b A) = G_b kA/(lh_b A) = G_b k/(lh_b) = 0.2616 \times 380/(2.5 \times 10^{-3} \times 2044.9) = 19.45.$$

(6) A finned tube augmentation factor can be easy expressed through a fin effectiveness E_f and a quotient δ/s by the following formula:

$$E_t = [E_f(\delta/s) + 1]/[(\delta/s) + 1] = [19.45(0.2/1) + 1]/[(0.2/1) + 1] = 4.074.$$

The input data and results of the whole calculation are collected in Table 1. Obtained values of the fin tube augmentation factor are presented in Fig. 10 by dot-centered open circles. The corresponding E_t curves for the same finned tube from Ünal's paper [7] are shown also in this figure. Our rather simple procedure using the ordinary functions is shown to give practically the same results as much more complex Ünal's method where a special function (Legendre's incomplete normal elliptic integral of the first kind) and corresponding table for modular angle 45° are used.

5. Conclusions

(1) Closed-form solution Eq. (1) of 1-D heat conduction problem for a straight fin with power-law-type temperature depending heat transfer coefficient is inverted into the recurrent expression Eq. (2) to determine T_e for given n and N. The recurrent formula (4) with very fast convergence is obtained by way of linearization of Eq. (2).
(2) A generalized expression for definite integral with respect to T depending on bottom limit of integration only (for given n) is found. It allows to find the inverse and direct formulae (12) and (13) for the temperature excess distribution throughout the fin.
(3) All obtained formulae at $n = 0$ transform to the well-known formulae for the fins with a uniform heat transfer coefficient.
(4) The approximations describing the limiting values of T_e^*, N^* and G_b^* are obtained for $-7 \leqslant n < -1$.
(5) Dimensionless thermal conductance G_b at the fin base is used in conjuction with obtained Eqs. (4)–(6) for T_e to calculate fins and finned surfaces.
(6) The relation $G_d = G_b/G_{b,0}$ for the relative fin base thermal conductance with any given value of n to that for $n = 0$ is introduced.
(7) Results of the evaluation based on the obtained formulae agree well with experimental data [4] on the pin fin temperature distribution in nucleate pool boiling with R113 ($n = 2$) and [5] in film pool boiling with water ($n = -0.5$). They also agree well with Ünal's theoretical determination [7] of the fin tube augmentation factor in pool nucleate boiling with R113 ($n = 2$).
(8) The obtained results allow to solve accurately in ordinary functions the different fin heat conduction problems which arise in practice including design and optimization of the fins and finned surfaces with power-law-type dependence of the heat transfer coefficient on the local temperature excess.

Acknowledgements

The authors thank Prof. Leonid M. Fisher, All-Russian Electrical Engineering Institute, Moscow, for the many helpful comments made on the manuscripts of [1] and the current paper.

Appendix A. The development procedure of the recurrent formula Eq. (4)

Analysis of Eq. (2) shows that this recurrent expression converges very slowly or does not converge for certain initial values of T_e. But a simple linearization of Eq. (2) allows to obtain a recurrent expression with very fast convergence for arbitrary initial value of $0 < T_e < 1$. Taking into account the denotation introduced in Eq. (5) $Z \simeq NT_e^{0.4n}$, Eq. (2) can be expressed in a form $T_e = 1/\cosh Z$. Let us denote an increment of T_e by Δ. Then

$$T_e + \Delta = \frac{1}{\cosh Z} - \frac{0.4nZ\tanh Z}{T_e \cosh Z}\Delta. \tag{A.1}$$

Taking into account the denotation introduced in Eq. (6) $A_z = 0.4nZ\tanh Z$ we get

$$\Delta = \frac{1 - T_e\cosh Z}{\cosh Z + A_z/T_e}. \tag{A.2}$$

Substituting Eq. (A.2) in Eq. (A.1) and taking into account that in an incremental form $T_{e,(j+1)} = T_{e,(j)} + \Delta$, where subscripts (j) and $(j+1)$ denote the iteration number, we finally get the following recurrent formula:

$$T_{e,(j+1)} = \frac{1 + A_z}{\cosh Z + A_z / T_{e,(j)}}, \qquad \text{(A.3)}$$

which is equivalent to Eq. (4).

References

[1] I.N. Dul'kin, G.I. Garas'ko, Analytical solutions of 1 D heat conduction problem for a single fin with temperature dependent heat transfer coefficient – I. Closed-form inverse solution, Int. J. Heat Mass Transfer 45 (2002) 1895–1903.

[2] K.A. Gardner, Efficiency of extended surface, Trans. ASME 67 (1945) 621–631.

[3] K.A. Gardner, in: Discussion in Proceedings of the General Discussion on Heat Transfer, Inst. Mech. Eng.-ASME, London, 1951, pp. 214–215.

[4] I.N. Dul'kin, Heat transfer with liquid boiling on a fin, Cand. Tech. Sci. Thesis, Moscow Power Engineering Institut (MEI), Moscow, 1974 (in Russian).

[5] S.P. Liaw, R.H. Yeh, Fins with temperature dependent surface heat flux-I. Single heat transfer mode, Int. J. Heat Mass Transfer 37 (1994) 1509–1515.

[6] A.D. Kraus, A.D. Snider, L.F. Doty, An efficient algorithm for evaluating arrays of extended surface, Trans. ASME Ser. C, J. Heat Transfer 100 (1978) 288–294.

[7] H.C. Ünal, A simple method of dimensioning straight fins for nucleate pool boiling, Int. J. Heat Mass Transfer 29 (1987) 640–644.